COBEM 2021 26th International Congress of Mechanical Engineering
November 22-26, 2021, Virtual Congress, Brazil
ABCM Associação Brasileira de Engenharia e Ciências Mecânicas

COB-2021-2326
Iterative Method to predict limit cycles in aeroelastic systems with freeplay and Coulomb friction via Describing Functions

Larissa Drews Wayhs-Lopes
Department of Mechanical Engineering, São Paulo State University (UNESP), School of Engineering of Ilha Solteira, 15385-000, SP, Brazil
larissa.d.wayhs@unesp.br

Douglas D. Bueno
Department of Mathematics, São Paulo State University (UNESP), School of Engineering of Ilha Solteira, 15385-000, SP, Brazil
douglas.bueno@unesp.br

Discontinuous nonlinearities are often present in aeroelastic systems. Particularly, freeplay and friction can change the dynamics of flight, leading the aircraft to limit cycle oscillations (LCO). The prediction of amplitude and frequency of LCO is an important task of engineers, since it can produce failure by fatigue. Typically, LCO are results of marginally stable conditions, characterized by the presence of zero real part of some eigenvalue of the dynamic matrix. Therefore, for linear systems, the search of LCO can be performed by classical linear stability analysis (eigenvalue problem). However, the discontinuity of piecewise nonlinearities produces difficulties to apply such analysis, since the dynamic matrix is no longer unique. A common solution to this problem is to employ the Equivalent Linearization Technique (ELT), where linear equivalent terms are obtained to properly represent the nonlinear system. In this context, this work presents the friction as a linear equivalent viscous damping and, because this equation is dependent on the LCO frequency, typically an output of the ELT, this work also proposes an iterative method to properly apply the ELT to the aeroelastic typical section with simultaneous freeplay and friction in control surface. The results show that the method is suitable for this condition.

Keywords: *Describing Function, Iterative Method, Equivalent Linearization Technique, Freeplay and Friction*

1. INTRODUCTION

Stability analysis of aeroelastic systems is an important topic considered to characterize the dynamics of flight of aerial vehicles. The presence of nonlinearities in control surfaces, such as freeplay and friction, can modify the aircraft stability, typically inducing limit cycle oscillations (LCO) (Dowell *et al.*, 2003). A common task of engineers is to predict the LCO conditions and determine their amplitude and frequency to properly define a safe flight envelope.

Typical methods often used to solve the linear stability analysis of an aeroelastic system involve eigenvalue problems, in which positive real part of an eigenvalue of aeroelastic dynamic matrix indicates instability (flutter). However, the presence of nonlinearities requires different strategies to evaluate the areoelastic stability. As a solution to this issue, a procedure called Equivalent Linearization Technique (ELT) is typically employed, in which a linear equivalent aeroelastic dynamic matrix is computed for each particular condition of the nonlinear system.

The Describing Function Method is often considered to obtain such linear equivalent matrix, since it aims to properly represent the nonlinear term with a linear equivalent expression. The approach involves the Fourier series to approximate the nonlinear term and it has been successfully employed to consider freeplay nonlinearity (Yang and Zhao, 1988; Price *et al.*, 1995; Tang *et al.*, 1998; Anderson and Mortara, 2007; Kholodar and Dickinson, 2010; Zhang and Wu, 2015; Yang *et al.*, 2016; He *et al.*, 2017; Padmanabhan and Dowell, 2017; Verstraelen *et al.*, 2017). On the other hand, Eller (2007) and Padmanabhan *et al.* (2018) introduce approaches to include friction forces with freeplay. However, their articles do not provide a detailed procedure to consider both nonlinearities and how their describing function-based method can be used to predict limit cycle oscillations.

In this context, this work introduces a describing function to represent the friction: the effect of friction torque is represented by a torque proportional to the velocity, written in terms of a linear equivalent viscous damping. In addition, considering that the math expression of the equivalent damping depends on the LCO frequency, the article also presents a new iterative approach involving the ELT to predict amplitude and frequency of LCO in aeroelastic system with freeplay and friction in the control surface. The article is focused on introducing the torques due to the freeplay and friction nonlinearities with their respective describing functions - and the detailed procedure to obtain them (section 2). Section 3. presents the Equivalent Linearization Technique and how it is adapted as an iterative method to consider both freeplay and

friction acting simultaneously. This last part is considered the most important contribution of the present work. Finally, the results of amplitude and frequency of LCO prediction for the typical section with control surface are presented in section 4. highlighting that it is important to consider the effect of friction. Using a proper time marching as a reference for the LCO prediction, the results show that the proposed iterative method is adequate to predict LCO for the system in such physical configuration.

2. FREEPLAY AND FRICTION WITH THEIR DESCRIBING FUNCTIONS

The symmetric freeplay can be evaluated such that the elastic restoring torque on the control surface hinge line is illustrated in Fig. 1a. and given by

$$f_l^{\delta}(t) = \begin{cases} k_{u_l}\left[u_l(t) + \delta\right] & , \quad u_l < -\delta \\ 0 & , \quad |u_l| < \delta \\ k_{u_l}\left[u_l(t) - \delta\right] & , \quad u_l > \delta \end{cases} \tag{1}$$

where the subscript l indicates the degree of freedom (DOF) associated to the freeplay. Similarly, the Coulomb friction is considered in such a way that an additional torque with amplitude c arises in the opposite direction to the motion of the same l-th DOF, given by

$$f_l^{c}(t) = \begin{cases} -c & , \quad \dot{u}_l < 0 \text{ and } |u_l| > \delta \\ 0 & , \quad |u_l| < \delta \\ c & , \quad \dot{u}_l > 0 \text{ and } |u_l| > \delta \end{cases} \tag{2}$$

where c is the amplitude of the Coulomb friction torque. See an illustrative representation in Fig. 1b.

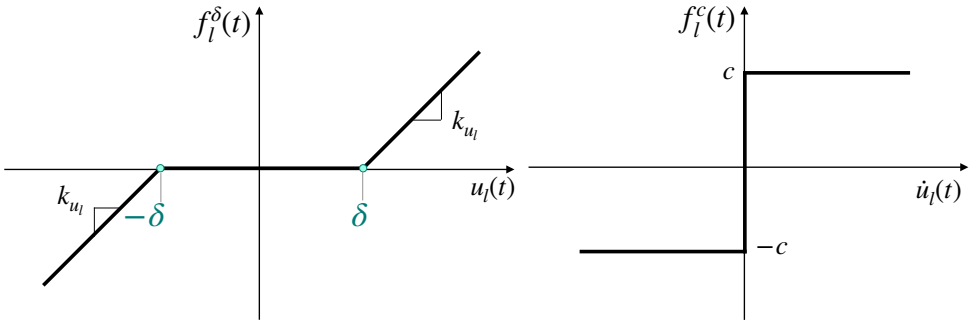

(a) Freeplay (b) Coulomb friction

Figure 1. Representation of nonlinearities effects (freeplay and Coulomb friction).

The aim of Describing Function Method is to properly represent the freeplay effects with a linear equivalent expression for stiffness ($\hat{k}_{u_l}$). The present article additionally proposes to include an equivalent viscous damping ($\hat{b}_{u_l}$) to describe the dissipative behavior of the friction torque. This is achieved by computing the harmonic balance for both sides of these linear equivalent torques $\hat{f}_l^{\delta} = \hat{k}_{u_l} u_l(t)$ and $\hat{f}_l^{c} = \hat{b}_{u_l} \dot{u}_l(t)$. For the freeplay, the left-hand side $\hat{f}_l^{\delta}$ approximates the nonlinear torque in Eq. (1) by the Fourier series - as illustrated in Fig. 2 - whilst the right-hand side is assumed as $u_l(t) = A_{u_l} \sin(\omega_{u_l} t)$ for describing a LCO with a single harmonic, where A_{u_l} and ω_{u_l} correspond to the amplitude and frequency of the motion, respectively. The friction torque is included using an analogous procedure, considering Eq. (2) to approximate by the Fourier series. Finally, solving for $\hat{k}_{u_l}$ and $\hat{b}_{u_l}$ by comparing the amplitudes of coefficients of each harmonic (i.e., performing the harmonic balance), it is obtained the equivalent linear stiffness and damping for a Fourier series of order p. In this work, $p = 1$ is considered. This procedure, properly detailed in subsection 2.1 allows one to obtain the describing function equations (DF), as shown in Eq. (3) and (4) for freeplay and friction, respectively. Note that the friction DF shows the combined effect of both friction and freeplay, since the nonlinear torque due to friction is affected by the freeplay (there is no friction inner the freeplay region).

$$\hat{k}_{u_l} = \frac{k_{u_l}}{\pi}\left[\pi - 2\theta_{\delta} - \sin(2\theta_{\delta})\right] \tag{3}$$

where $\theta_{\delta} = \sin^{-1}(\delta / A_{u_l})$

$$\hat{b}_{u_l} = \frac{4c}{\pi A_{u_l} \omega_{u_l}}\left[1 - \frac{\delta}{A_{u_l}}\right] \tag{4}$$

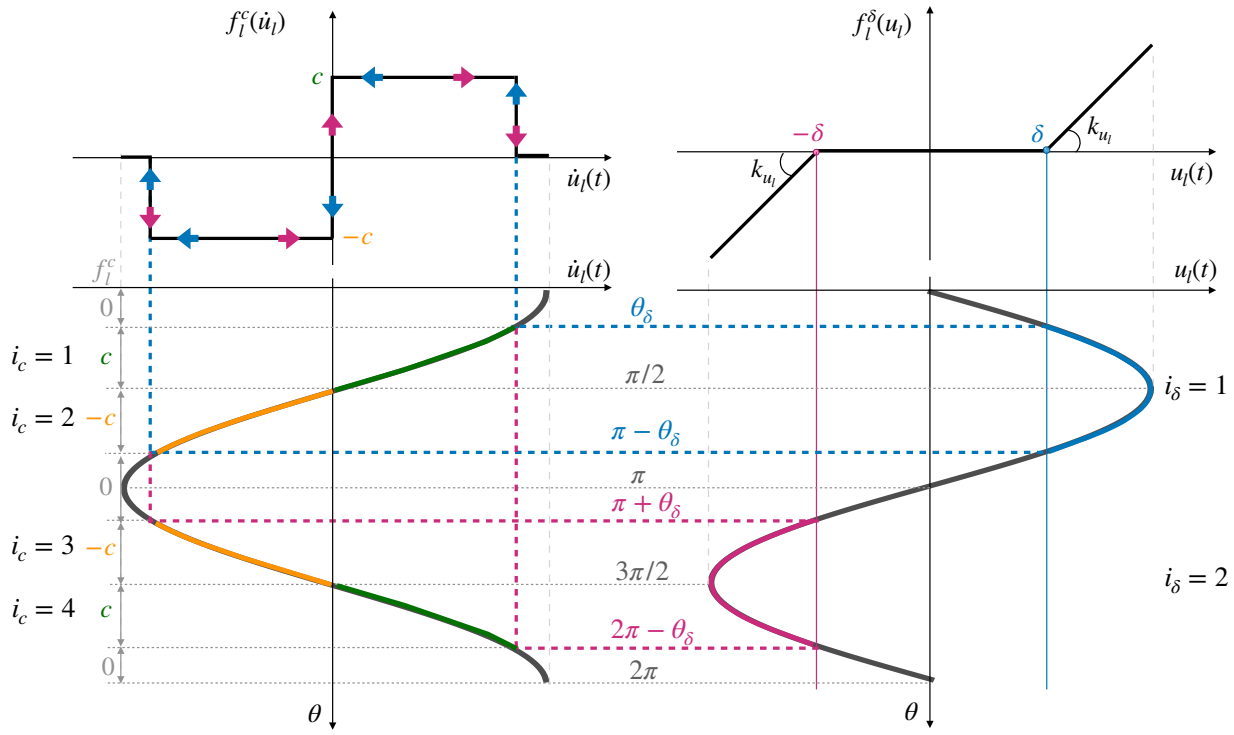

Figure 2. Scheme of nonlinear torques as an aid to perform the Fourier Series.

2.1 Computing Describing Functions

This appendix shows details of computing the coefficients of Fourier series (presented in Eq. 5 and 6) considering a truncate series of order p. The specific final expression for these coefficients are presented for the case of considering only the first harmonic, i.e., $p = 1$. Considering that there are $N_{reg} = 2$ linear regions of nonlinear torque f_l^ϵ in which $f_l^\epsilon \neq 0$ for freeplay and $N_{reg} = 4$ for friction (see Eq. (1), (2) and Fig. 2), the Tab. 1 and 2 present the values of θ_{i_1}, θ_{i_2} and $f_{l,i}^\epsilon(t)$ with their parameters for each region i to be integrated, respectively for freeplay and friction. The general expressions for $\bar{A}_{n,i}^\epsilon$ and $\bar{B}_{n,i}^\epsilon$, which are part of the coefficients of order n in Eq. (7), are presented in Eq. from (8) to (9) for freeplay and friction of order 1. Finally, applying Eq. (8) and (9) in Eq. (7), and then employing in Eq. (5) and (6), the DF equations (3) and (4), respectively, are obtained.

$$\hat{k}_{u_l} = \left| \frac{\mathcal{F}_s(f_l^\delta)_p}{A_{u_l} \sin(\omega_{u_l} t)} \right| = \frac{1}{A_{u_l}} \sqrt{\sum_{n=1}^{p} \left(A_{\delta,n}^2 + B_{\delta,n}^2 \right)} \tag{5}$$

$$\hat{b}_{u_l} = \left| \frac{\mathcal{F}_s(f_l^c)_p}{A_{u_l} \omega_{u_l} \cos(\omega_{u_l} t)} \right| = \frac{1}{A_{u_l} \omega_{u_l}} \sqrt{\sum_{n=1}^{p} \left(A_{c,n}^2 + B_{c,n}^2 \right)} \tag{6}$$

where $A_{\delta,n}$, $B_{\delta,n}$, $A_{c,n}$ and $B_{c,n}$ are the coefficients of Fourier series.

$$A_{\epsilon,n} = \frac{1}{\pi} \sum_{i=1}^{N_{reg}} \bar{A}_{n,i}^\epsilon \qquad B_{\epsilon,n} = \frac{1}{\pi} \sum_{i=1}^{N_{reg}} \bar{B}_{n,i}^\epsilon$$

where, (7)

$$\bar{A}_{n,i}^\epsilon = \int_{\theta_{i_1}}^{\theta_{i_2}} f_{l,i}^\epsilon(t) \cos(n\theta) d\theta \qquad \bar{B}_{n,i}^\epsilon = \int_{\theta_{i_1}}^{\theta_{i_2}} f_{l,i}^\epsilon(t) \sin(n\theta) d\theta$$

where i refers to each one of these regions. This is valid for freeplay ($\epsilon = \delta$) or friction ($\epsilon = c$).

$$\begin{aligned} \bar{A}_{1,i}^\delta &= \bar{f}_i [\sin\theta_{i_2} - \sin\theta_{i_1}] + \frac{\bar{k}_i A_{u_l}}{2} [\sin^2\theta_{i_2} - \sin^2\theta_{i_1}] \\ \bar{B}_{1,i}^\delta &= \bar{f}_i [\cos\theta_{i_1} - \cos\theta_{i_2}] + \frac{\bar{k}_i A_{u_l}}{2} \left[\theta_{i_2} - \theta_{i_1} - \frac{(\sin 2\theta_{i_2} - \sin 2\theta_{i_1})}{2} \right] \end{aligned} \tag{8}$$

Table 1. Parameters of the nonlinear torque due to freeplay of each region from 0 to 2π: $f_{l,i}^{\delta}(t) = \bar{f}_i + \bar{k}_i u_l(t)$, where $\bar{f}_i = f_{0,i} - \bar{k}_i u_{l0,i}$

Region $i = i_\delta$	θ_{i_1}	θ_{i_2}	$f_{0,i}$	$u_{l0,i}$	k_i
1	θ_δ	$\pi - \theta_\delta$	0	δ	k_{u_l}
2	$\pi + \theta_\delta$	$2\pi - \theta_\delta$	0	$-\delta$	k_{u_l}

where $f_{0,i}$ and $u_{l0,i}$ are the torque and the displacement on the beginning of linear region i, whose stiffness (slope) is $\bar{k}_i$ and the motion is $u_l(t) = A_{u_l} \sin\theta$ (see Eq. 1)

Table 2. Parameters of the nonlinear torque due to friction of each region from 0 to 2π: $f_{l,i}^{c}(t) = f_{c,i}$

Region $i = i_c$	θ_{i_1}	θ_{i_2}	$f_{c,i}$
1	θ_δ	$\pi/2$	c
2	$\pi/2$	$\pi - \theta_\delta$	$-c$
3	$\pi + \theta_\delta$	$3\pi/2$	$-c$
4	$3\pi/2$	$2\pi - \theta_\delta$	c

$f_{c,i}$ is the torque due to friction, in region i (see Eq. 2)

$$\begin{aligned} \bar{A}_{1,i}^{c} &= f_{c,i}(\sin\theta_{i_2} - \sin\theta_{i_1}) \\ \bar{B}_{1,i}^{c} &= f_{c,i}(\cos\theta_{i_1} - \cos\theta_{i_2}) \end{aligned} \tag{9}$$

3. EQUIVALENT LINEARIZATION TECHNIQUE

The classic linear stability analysis for a linear system described by the state space notation is performed by extracting the eigenvalues of the aeroelastic dynamic matrix $\mathbf{A}$ to evaluate their real part. On the other hand, the presence of freeplay or friction produces a piecewise linear system. Then, the LCO conditions for the nonlinear system correspond to the marginally stable conditions of the linear equivalent system. In practice, a dynamic matrix is defined for all possible values of linear equivalent stiffness $0 < \hat{k}_{u_l} < k_{u_l}$ and for each value of the linear damping coefficient, such that

$$\hat{\mathbf{A}} = \hat{\mathbf{A}}(V, \hat{\mathbf{K}}, \hat{\mathbf{D}}) \tag{10}$$

where the structural stiffness and damping equivalent matrices $\hat{\mathbf{K}}$ and $\hat{\mathbf{D}}$ are dependent on $\hat{k}_{u_l}$ and $\hat{b}_{u_l}$ in such a way that they are exact copies of the matrices $\mathbf{K}$ and $\mathbf{D}$ of the original overlying system (outside of freeplay - see appendix A) with the exception that the equivalent values $\hat{k}_{u_l}$ and $\hat{b}_{u_l}$ are placed on the l-th row and l-th column of their respective matrices.

The main idea to apply the ELT considering freeplay is to associate a linear equivalent system at the same flight condition (i.e., velocity and density), and the key point is considering the following associations: i. each equivalent stiffness $\hat{k}_{u_l}$ is used in the linear equivalent dynamic matrix $\hat{\mathbf{A}}$ and it is, therefore, associated with pairs of airspeed and frequency ($V_{g=0},\ f_{g=0}$), corresponding to the marginally stable condition through the eigenvalue of $\hat{\mathbf{A}}$; ii. each equivalent stiffness is also associated with an amplitude A_{ul} of motion via the describing function of Eq. (3), for each particular freeplay δ. Then, it is possible to associate the pairs ($V_{g=0},\ f_{g=0}$) with an amplitude of motion A_{u_l}. The prediction indicates that, at speed $V_{g=0}$, the motion occurs with amplitude A_{u_l} and frequency $\omega_{u_l} = 2\pi f_{g=0}$, which allows one to characterize the LCO condition.

There is an important challenge for applying the procedure described above if freeplay and friction are considered simultaneously because the DF for friction (see Eq. (4)) depends on the oscillation frequency ω_{u_l}. Note that the classical ELT using DFs considers the oscillatory frequency as an output once it is obtained from the eigenvalue (i.e., the imaginary part of the eigenvalue with zero real part). The issue is that the frequency is required to compute the equivalent damping $\hat{b}_{u_l}$, which is used to define the matrix $\hat{\mathbf{A}}$ to extract the eigenvalues. Then, this work proposes the iterative method illustrated in Fig. 3. In practice, for a pair of freeplay δ and friction c, and for each equivalent stiffness in the range $0 < \hat{k}_{u_l} < k_{u_l}$, the following sequence is employed:

1. Use δ, $\hat{k}_{u_l}$ and k_{u_l} to compute A_{u_l} via Eq. (3);
2. Choose an initial guess $\omega_{u_l} = \omega^0$ for the frequency (a good guess is the frequency obtained for the ELT for the system only with freeplay for the current equivalent stiffness);
3. Use δ, c, A_{u_l} (from step 1) and ω_{u_l} to compute $\hat{b}_{u_l}$ via Eq. (4);

4. Use the current $\hat{k}_{u_l}$ and $\hat{b}_{u_l}$ from step 3 to run the liner stability analysis (i.e., for a given speed range, the linear equivalent dynamic matrix $\hat{\mathbf{A}}$ (see Eq. 10) is computed and their eigenvalues are extracted in search for a marginally stable condition) to find some pair of speed and frequency $(V_{g=0},\ f_{g=0})$;

5. Check whether the stop criterion $|2\pi f_{g=0} - \omega_{u_l}| < \epsilon$ is achieved, for tolerance ϵ.

   - if not: update the frequency to $\omega_{u_l} = 2\pi f_{g=0}$ and go to step 3.
   - if yes: the process for searching for this specific pair $(V_{g=0},\ f_{g=0})$ for the current $\hat{k}_{u_l}$ is finished and the process is continued through the speed range until all pairs $(V_{g=0},\ f_{g=0})$ for this $\hat{k}_{u_l}$ have been found and converged satisfying the given tolerance.

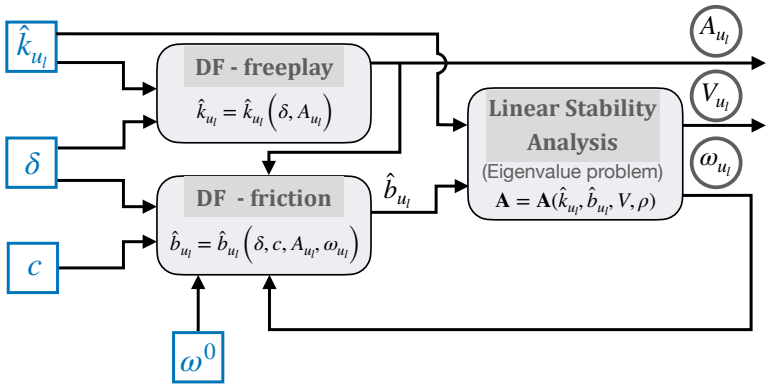

Figure 3. Iterative process to apply the Equivalent Linearization Technique combined with a describing function if freeplay and friction are considered to predict LCOs.

4. RESULTS

The typical section with three degree-of-freedom (DOF) is modeled such that plunge (h) and pitch of wing (θ) are linear DOFs and the control surface rotation (β) is considered with freeplay and friction, according to Fig. 4. The displacement vector is $\mathbf{u} = \{h \quad \theta \quad \beta\}^T$, for which the nonlinear DOF $u_l = \beta$ is placed at the row $l = 3$. The equation of motion for the nonlinear system with freeplay and friction is $\dot{\mathbf{x}} = \mathbf{A}^f\mathbf{x} - \mathbf{b}^\delta - \mathbf{b}^c$, such that $\mathbf{b}^\delta = \left\{\mathbf{M}_a^{-1}\mathbf{f}^\delta\ 0\ ...\ 0\right\}^T$ and $\mathbf{b}^c = \left\{\ \mathbf{M}_a^{-1}\mathbf{f}^c\ 0\ ...\ 0\right\}^T$ are $N \times 1$ vectors, whereas $\mathbf{f}^\delta$ and $\mathbf{f}^c$ are $n \times 1$ null vectors with f_l^δ and f_l^c in the l-th row. Note that both f_l^δ and f_l^c have unities of torque per unit of span (Nm/m) because the aeroelastic equation of motion for the typical section where they are inserted is typically written per unit of span. The nominal stiffness k_β and other parameters and matrices are presented in Appendix A.

Figure 5 shows the classical V-g-f diagram for the linear nominal system (i.e., the system with no freeplay neither friction) obtained by the classic stability analysis, which shows that the velocity and frequency of flutter, are respectively $V_f = 47,09$ m/s and $f_f = 5,62$ Hz. Note that the flutter occurs at the lowest velocity condition for which there is a marginally stable condition, i.e., when some of the complex eigenvalues of matrix $\mathbf{A}$ has a null real part.

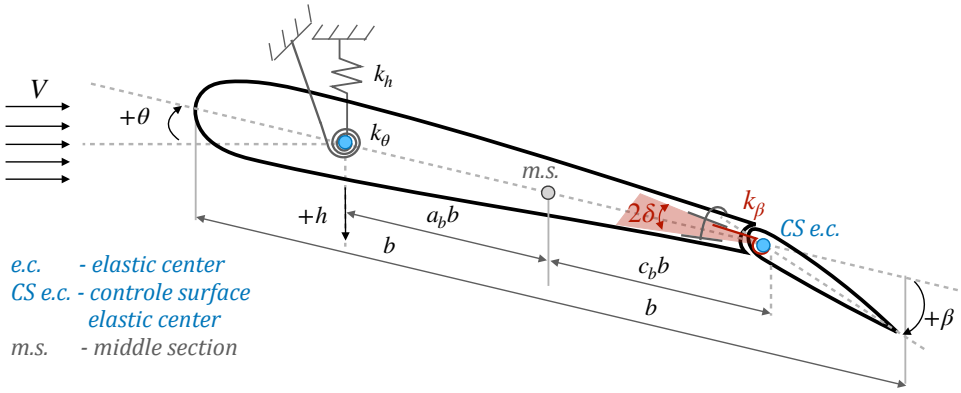

Figure 4. Three DOF typical section with control surface freeplay.

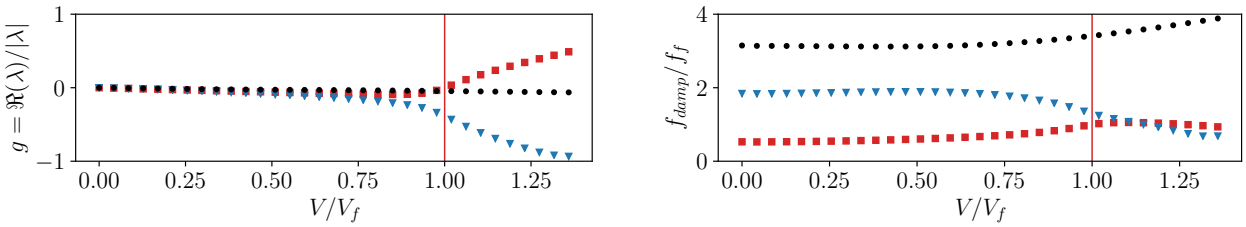

Figure 5. V-g and V-f diagrams, where $g = \Re(\lambda)/|\lambda|$ and $f_{damp} = \Im(\lambda)$, for λ being the eigenvalue of the linear matrix $\mathbf{A}$ (the dynamic matrix considering k_β, i.e., overlying system): plunge mode (■), pitch mode (▼), control surface rotation mode (●). The vertical line indicates the flutter velocity $V_f = 47,09$ m/s.

The range of equivalent stiffness $\hat{k}_\beta$ is defined between 0% and 100% of nominal stiffness k_β - i.e., $0 < (\hat{k}_\beta/k_\beta) < 1$. For the system containing only freeplay, it is possible to perform the ELT without considering the iterative method, as detailed on second paragraph of section 3. It means that, the range of air velocity is covered to find all marginally stable conditions $(V_{g=0}, f_{g=0})$ for each equivalent stiffness. This stage is the association i. referred in section 3, where each equivalent stiffness $\hat{k}_\beta$ (x-axis) when employed on matrix $\hat{\mathbf{A}}$ is related to some velocities $V_{g=0}$ (y-axis of Fig. 6 a.) for which some eigenvalue has $g = 0$ and whose imaginary part is the frequency $f_{g=0}$ (y-axis of Fig. 6 b.). In addition, the association ii. between $\hat{k}_\beta$ and the amplitude A_β of LCO is performed by using the DF shown in Eq. (3) (see Fig. 7). Note that the horizontal line in this figure indicates the limit value of $A_\beta/\delta = 1$ for which the expression of describing function is mathematically valid. Finally, relating the results of Fig. 6 (values of $V_{g=0}$ and $f_{g=0}$) and Fig. 7 (values of A_β) for each given equivalent stiffness, it is possible to obtain the final prediction of LCO, i.e., the amplitude A_β and frequency $f_{g=0}$ occurring in the air velocity condition $V_{g=0}$. This is a well-known procedure to LCO prediction if only freeplay is considered, and the results are shown in Fig. 8. The Hénon's Technique (Wayhs-Lopes *et al.*, 2020) is employed to perform time integration of the nonlinear system to compare and validate the results, which demonstrates that the approach predicts LCO accurately.

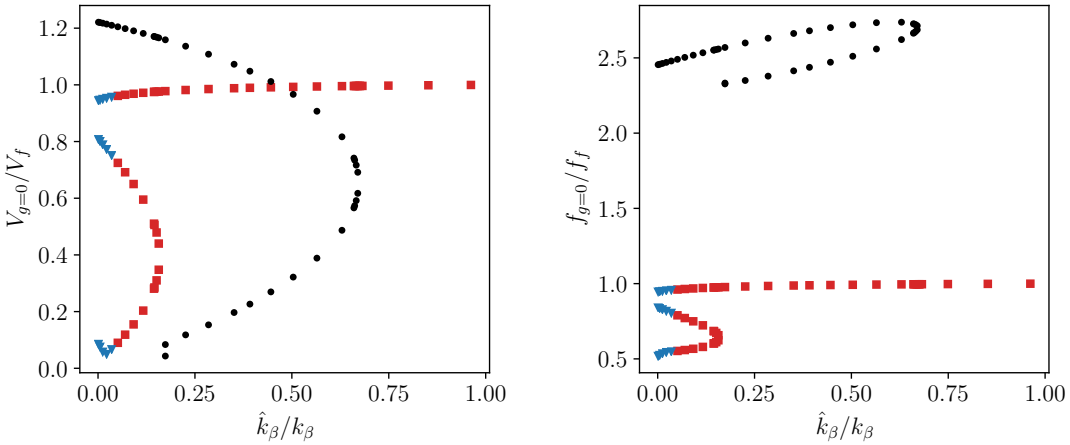

Figure 6. Marginally stable conditions $(V_{g=0}, f_{g=0})$ obtained via ELT in terms of the equivalent stiffness $\hat{k}_\beta$ - no friction. Symbols indicate the mode associated with the eigenvalue with $g = 0$: plunge (■), pitch (▼), control surface rotation (●).

Considering both freeplay and friction, the same range of equivalent stiffness is assumed to employ the required iterative ELT presented in section 3. Note that the results relating equivalent stiffness with LCO amplitude (obtained via Eq. (3)) shown in Fig. 7 are the same results obtained with no friction. However, the main difference consists to the stage related to the correlation of the equivalent stiffness with each pair $(V_{g=0}, f_{g=0})$. Therefore, after performing the iterative ELT for two cases of friction ($c = 1.25\ 10^{-3}$ and $c = 3.75\ 10^{-3}$ Nm /m) it is finally possible to relate a pair $(V_{g=0}, f_{g=0})$ in Fig. 9 with the LCO amplitude A_β shown in Fig. 7, which allows one to obtain the LCO prediction shown in Fig. 10. The results show that this proposed method is suitable to predict LCO for systems with both freeplay and friction acting in the same DOF. It is important to highlight that if there is friction, but is not taken into account on the LCO prediction, the classical ELT (with no iterative procedure) provides inaccurate results.

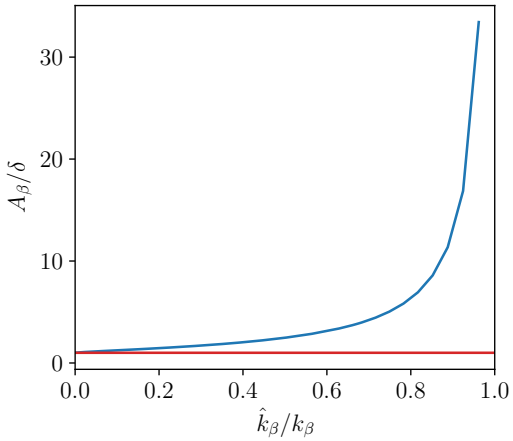

Figure 7. Amplitude of LCO A_β via freeplay DF (Eq. 3) in terms of the equivalent stiffness $\hat{k}_\beta$.

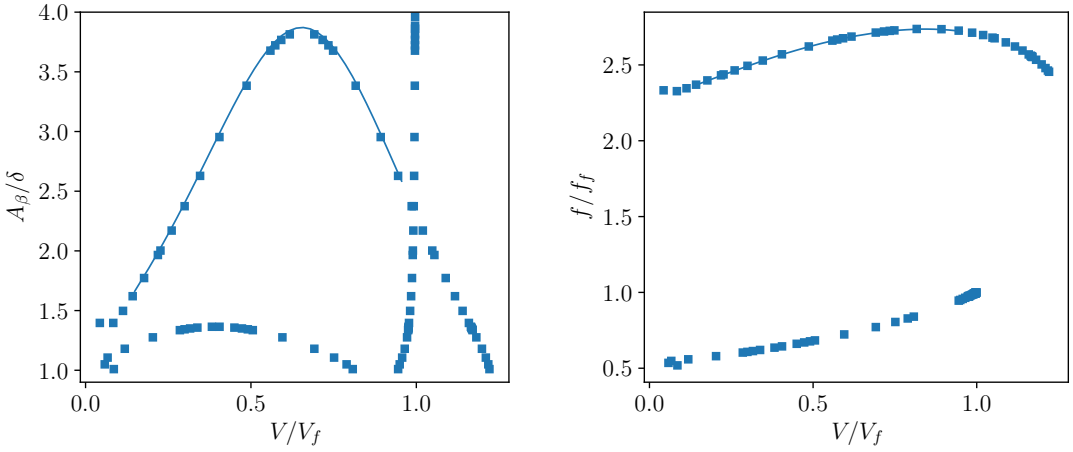

(a) (b)

Figure 8. Prediction of (a) amplitude and (b) frequency of all possible LCO conditions via ELT, for the system with only freeplay $\delta = 0.5$ deg. Symbols for ELT (■) and solid line for time integration as reference (—).

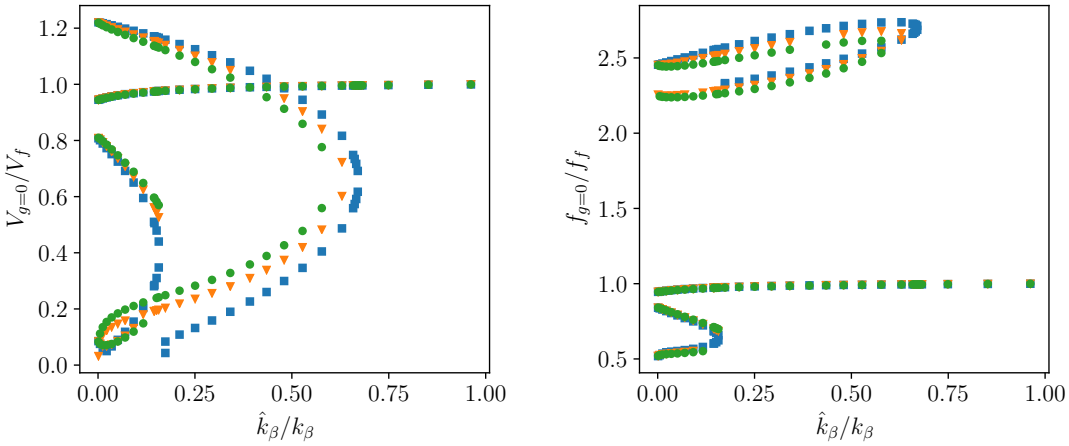

Figure 9. Marginally stable conditions ($V_{g=0}$, $f_{g=0}$) obtained via ELT (with iterative procedure in the cases with friction) in terms of the equivalent stiffness $\hat{k}_\beta$. No friction (■); $c = 1.25\ 10^{-3}$ Nm /m (▼); $c = 3.75\ 10^{-3}$ Nm /m (●).

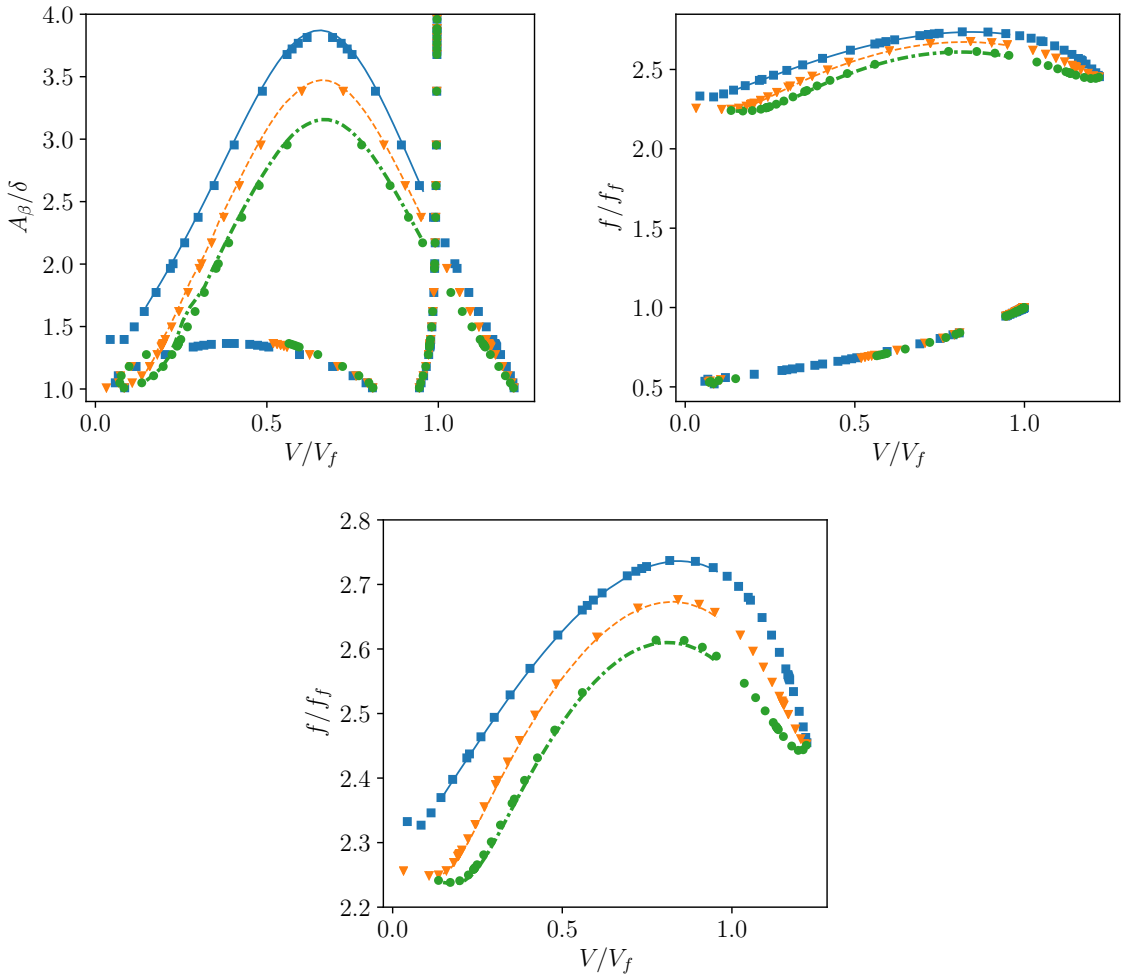

Figure 10. Prediction of amplitude and frequency - with zoom in the last subfigure - of all possible LCO conditions via ELT employing iterative procedure, for the system with simultaneous freeplay ($\delta = 0.5$ deg) and friction. Legend: symbols for ELT and lines for time integration as referece (H). No friction (■, solid line —); $c = 1.25\ 10^{-3}$ Nm /m (▼, dashed line - - -); $c = 3.75\ 10^{-3}$ Nm /m (●, dash-dotted line - · -).

5. FINAL REMARKS

This work introduced the procedure to obtain a linear equivalent equation named describing functions corresponding to the stiffness to describe the freeplay nonlinearity. It is also proposed a new approach to represent the effect of Coulomb friction introducing a linear equivalent viscous damping. The new DF is dependent on the LCO frequency, and because of this, the present work introduced an iterative procedure to employ the Equivalent Linearization Technique in aeroelastic system presenting simultaneous freeplay and friction. The results show that this method is suitable to predict frequency and amplitude of LCO for which the motion presents only the first harmonic as predominant.

6. ACKNOWLEDGEMENTS

The first author would like to thank SÃčo Paulo Research Foundation (FAPESP), Grant number 2019/22730-7.

7. REFERENCES

Anderson, W.D. and Mortara, S., 2007. "Maximum control surface freeplay, design and flight testing approach on the f-22". In *AIAA Paper 07-1767, AIAA/ASME/ASCE/ AHS/ASC Structures, Structural Dynamics, and Materials Conference*.

Dowell, E., Edwards, J. and Strganac, T., 2003. "Nonlinear aeroelasticity". *Journal of Aircraft*, Vol. 40, No. 5, pp. 857–874. doi:10.2514/2.6876.

Eller, D., 2007. "Friction, freeplay and flutter of manually controlled aircraft". In *IFASD - International Forum on*

Aeroelasticity and Structural Dynamics.

He, S., Yang, Z. and Gu, Y., 2017. "Nonlinear dynamics of an aeroelastic airfoil with free-play in transonic flow". *Nonlinear Dynamics*, Vol. 87, No. 4, pp. 2099–2125. doi:10.1007/s11071-016-3176-4.

Kholodar, D. and Dickinson, M., 2010. "Aileron freepaly". In *International Forum of Aeroelasticity and Structural Dynamics - IFASD*.

Padmanabhan, M. and Dowell, E., 2017. "Calculation of aeroelastic limit cycles due to localized nonlinearity and static preload". *AIAA Journal*, Vol. 55, pp. 1–11. doi:10.2514/1.J055505.

Padmanabhan, M., Dowell, E. and Pasiliao, C., 2018. "Computational study of aeroelastic limit cycles due to localized structural nonlinearities". *Journal of Aircraft*, Vol. 55, pp. 1–11. doi:10.2514/1.C034645.

Price, S., Alighanbari, H. and Lee, B., 1995. "The aeroelastic response of a two-dimensional airfoil with bilinear and cubic structural nonlinearities". *Journal of Fluids and Structures*, Vol. 9, No. 2, pp. 175 – 193. ISSN 0889-9746. doi:https://doi.org/10.1006/jfls.1995.1009.

Roger, K., 1977. "Airplane math modelling methods for active control design". *AGARD Conference Proceeding*, Vol. 9, pp. 4.1–4.11.

Tang, D., Dowell, E.H. and Virgin, L.N., 1998. "Limit cycle behaviour of an airfoil with a control surface". *Journal Fluids and Structures*, Vol. 12, pp. 839–858.

Theodorsen, T., 1935. "General theory of aerodynamic instability and the mechanism of flutter". *NACA Rept. 496*, Vol. 13, pp. 374–387.

Verstraelen, E., Dimitriadis, G., Rossetto, G.D.B. and Dowell, E.H., 2017. "Two-domain and three-domain limit cycles in a typical aeroelastic system with freeplay in pitch". *Journal of Fluids and Structures*, Vol. 69, pp. 89 – 107. ISSN 0889-9746. doi:https://doi.org/10.1016/j.jfluidstructs.2016.11.019.

Wayhs-Lopes, L.D., Dowell, E.H. and Bueno, D.D., 2020. "Influence of friction and asymmetric freeplay on the limit cycle oscillation in aeroelastic system: An extended hÃl'nonâĂŹs technique to temporal integration". *Journal of Fluids and Structures*, Vol. 96, p. 103054. ISSN 0889-9746. doi:https://doi.org/10.1016/j.jfluidstructs.2020.103054.

Yang, Z. and Zhao, L., 1988. "Analysis of limit cycle flutter of an airfoil in incompressible flow". *Journal of Sound and Vibration*, Vol. 123, No. 1, pp. 1 – 13. ISSN 0022-460X. doi:https://doi.org/10.1016/S0022-460X(88)80073-7.

Yang, Z., He, S. and Gu, Y., 2016. "Transonic limit cycle oscillation behavior of an aeroelastic airfoil with free-play". *Journal of Fluids and Structures*, Vol. 66, pp. 1 – 18. ISSN 0889-9746. doi:https://doi.org/10.1016/j.jfluidstructs.2016.07.013.

Zhang, H. and Wu, J., 2015. "The aeroelastic characteristic of a wing with preload asymmetry freeplay". *Procedia Engineering*, Vol. 99. doi:10.1016/j.proeng.2014.12.507.

8. RESPONSIBILITY NOTICE

The authors are solely responsible for the printed material included in this paper.

Appendices

A The 3-DOF Typical Section

This appendix shows the dynamic matrix (Eq. 11) of the overlying system (outside of freeplay, with nominal stiffness) and submatrices (Eq. 12) used to define the state space model of the typical section of Theodorsen (1935). The Roger's approximation is used to write the unsteady aerodynamic forces in the time domain (Roger, 1977).

$$\mathbf{A} = \begin{bmatrix} [\bar{\mathbf{A}}]_{2n \times 2n} & [\bar{\mathbf{Q}}]_{2n \times n_{lag}n} \\ [\bar{\mathbf{I0}}]_{n_{lag}n \times 2n} & [\bar{\mathbf{\Gamma}}]_{n_{lag}n \times n_{lag}n} \end{bmatrix}_{N \times N} \tag{11}$$

$$\begin{gathered} \bar{\mathbf{A}} = \begin{bmatrix} -\mathbf{M}_a^{-1}\mathbf{D}_a & -\mathbf{M}_a^{-1}\mathbf{K}_a \\ \mathbf{I}_n & \mathbf{0}_{n\times n} \end{bmatrix} \quad \bar{\mathbf{Q}} = \begin{bmatrix} q\mathbf{M}_a^{-1}\mathbf{Q}_{1+2} & \dots & q\mathbf{M}_a^{-1}\mathbf{Q}_{(n_{lag}+2)} \\ \mathbf{0}_{n\times n} & \dots & \mathbf{0}_{n\times n} \end{bmatrix} \\ \bar{\mathbf{I0}} = \begin{bmatrix} \mathbf{I}_n & \mathbf{0}_{n\times n} \\ \vdots & \vdots \\ \mathbf{I}_n & \mathbf{0}_{n\times n} \end{bmatrix} \qquad \mathbf{\Gamma} = -\frac{V}{b}\begin{bmatrix} \gamma_1\mathbf{I}_n & \dots & \mathbf{0}_{n\times n} \\ \vdots & \ddots & \vdots \\ \mathbf{0}_{n\times n} & \dots & \gamma_{n_{lag}}\mathbf{I}_n \end{bmatrix} \end{gathered} \tag{12}$$

and, also,

$$\mathbf{M}_a = \mathbf{M} - q\left(\frac{b}{V}\right)^2\mathbf{Q}_2 \quad ; \quad \mathbf{D}_a = \mathbf{D} - q\left(\frac{b}{V}\right)\mathbf{Q}_1 \quad ; \quad \mathbf{K}_a = \mathbf{K} - q\mathbf{Q}_0 \tag{13}$$

This present study considers the 3 degree-of-freedom airfoil for which the matrix of mass is given by

$$\mathbf{M} = \begin{bmatrix} m & S_\theta & S_\beta \\ S_\theta & I_\theta & I_\beta + b(c_b - a_b)S_\beta \\ S_\beta & I_\beta + b(c_b - a_b)S_\beta & I_\beta \end{bmatrix}; \qquad \mathbf{K} = \mathrm{diag}(k_h,\ k_\theta,\ k_\beta) \tag{14}$$

where m is the mass, b is the aerodynamic semichord, I_θ and S_θ are the inertia and static moments of mass of wing-aileron around elastic center of wing ($e.c.$); I_β and S_β are the inertia and static moments of mass of aileron around elastic center of aileron ($e.c.^\beta$). $\mathbf{K}$ is the stiffness matrix of the overlying system, with the nominal stiffness k_β placed on the 3rd row and 3rd column. Note that $u_l = \beta$ and $\dot{u}_l = \dot{\beta}$. The linear equivalent matrix $\hat{\mathbf{K}} = \mathrm{diag}(k_h, k_\theta, \hat{k}_\beta)$ is employed in Eq. (13) instead of $\mathbf{K}$ to compute the linear equivalent aeroelastic matrix $\hat{\mathbf{A}}$ (instead of $\mathbf{A}$), used to the equivalent linear stability analysis on the Equivalent Linearization Technique (ELT). Also, the structural damping matrix $\mathbf{D}$ is assumed to be zero, and, a linear equivalent $\hat{\mathbf{D}} = \mathrm{diag}(0, 0, \hat{b}_\beta)$ is defined to employ the iterative procedure of ELT. Similar procedure is performed to obtain the dynamic matrix $\mathbf{A}^f$ used in time integration, where $\hat{k}_\beta = 0$ and $\hat{b}_\beta = 0$ are adopted. The displacement vector is $\mathbf{u}(t) = \{h(t)\ \theta(t)\ \beta(t)\}^T$ (i.e., the plunge, pitch and control surface rotation, respectively) with dimension $n \times 1$, for $n = 3$. The unsteady aerodynamics of Theodorsen (1935) are used with $n_{lag} = 7$ lag states in a rational function approximation ($\gamma_1 = 0.05$, $\gamma_2 = 0.21$, $\gamma_3 = 0.48$, $\gamma_4 = 0.85$, $\gamma_5 = 1.33$, $\gamma_6 = 1.91$ and $\gamma_7 = 2.60$). Also, the state vector is $\mathbf{x} = \{\dot{\mathbf{u}} \quad \mathbf{u} \quad \mathbf{u}_{lag}\}^T$ has dimension $N \times 1$, for $N = n(2 + n_{lag})$ and $\mathbf{u}_{lag}$ is a $nn_{lag} \times 1$ vector containing the inflow states arising from the rational function used in Roger's approximation. The air density is 1.225 kg/m^3 and the other parameters are shown in Table 3.

Table 3. Physical and geometric parameters for the three DOF typical section

Span	$s = 0.5$ m
Semi-chord	$b = 0.15$ m
Total mass (per unit of span)	$m = 7.5122$ kg/m
Non-dimensional distance* (w.r.t b) from $m.s.$ to $e.c.$	$a_b = -0.4$
Non-dimensional distance (w.r.t b) from $m.s.$ to $e.c.^\beta$	$c_b = 0.6$
Inertia moment (per unit of span) of wing-aileron around $e.c.$	$I_\theta = 4.7741\ 10^{-2}$ kgm^2 /m
Inertia moment (per unit of span) of aileron around $e.c.^\beta$	$I_\beta = 3.6423\ 10^{-4}$ kgm^2 /m
Static moment (per unit of span) of wing-aileron around $e.c.$	$S_\theta = 0.276426$ kgm/m
Static moment (per unit of span) of aileron around $e.c.^\beta$	$S_\beta = 0.011187$ kgm/m
Stiffness in plunge h (per unit of span)	$k_h = 2669.12$ (N/m)/m
Stiffness in pitch θ (per unit of span)	$k_\theta = 188.47$ (N/rad)/m
Stiffness in β (per unit of span)	$k_\beta = 2.82$ (N/rad)/m

*Positive value to the right-hand side of middle section ($m.s.$) and negative to the left-hand side of $m.s.$.